



IMPLEMENTATION OF AN ACOUSTIC STALL DETECTION SYSTEM USING NEAR- FIELD DIY PRESSURE SENSORS

Alessandro CORSINI^{1,2}, Sara FEUDO¹, Anthony G. SHEARD³,
Cecilia TORTORA¹, Graziano ULLUCCI²

¹ *Dipartimento di Ingegneria Meccanica e Aerospaziale, Sapienza University of Rome,
Via Eudossiana 18, Rome, Italy*

² *SED Soluzioni per l'Energia e la Diagnostica, Ferentino (FR), Italy*

³ *Fläkt Woods Limited, Axial Way, Colchester CO4 5AR, UK*

SUMMARY

In this paper the authors propose the use of an unconventional instrumentation, based on a DIY transducer, to measure the pressure instabilities in a low speed industrial axial fan, with the purpose of rotating stall detection. Rotating stall is an aerodynamic instability with a frequency typically half the rotor frequency, and in slow turbomachines such as industrial fans this frequency has a value even lower than 10 Hz.

The authors carried out the pressure measurements using a dynamic transducer and a piezoelectric sensor to provide the measurement base-line. In turbomachinery standard methods, time-resolved pressure measurements use piezoelectric sensors such as microphones in the far field and pressure transducers in the near field. Other classes of sensors, such as electret microphones, may be not suited for pressure measurements, especially in the infrasound region since their cut-off frequency is about 20 Hz.

In the present study, the authors compare a low cost and DIY technology to a high precision piezoelectric sensor as alternative technology to stall detection. They implemented and set-up a measurement chain that is the basis of a stall warning system able to identify the rotating stall typical pattern in low speed axial fans. The results have been validated respect to the state of the art of the acoustic control techniques described in literature.

The signals acquired using the two technologies are discussed combining spectral analysis and time-domain reconstruction of phase space portraits. The acoustic patterns obtained through the phase space reconstruction shows that the DIY dynamic sensor is a good candidate solution for the rotating stall acoustic analysis.

INTRODUCTION

The prediction of aerodynamic instabilities, such as rotating stall, is an important topic relevant to design and operation of industrial turbomachinery. In the past decades the rotating stall and its propagation mechanism were widely observed and studied (1). These phenomena were of primary designer interest as a consequence of the linked vibrational issues, leading to fatigue breakage of rotor blades. In this respect, the continuous machine monitoring is considered to be a remedial strategy able to detect the instabilities for timely intervention.

This paper reports on the identification of the rotating stall by means of the signals of the sound pressure emitted from an axial fan at low speed of the industrial type. The aerodynamic instability are hydrodynamically detectable in the near-field, and acoustically since each turbomachine emits noise due to the high speed of the flow thorough the rotating blades and stationary vanes in the duct, the intensity of the noise depends on the speed of rotation of the blades and the position of these objects (2, 3), this means that any divergence of the flow by the stability has as a consequence a change in the noise emitted.

The available technologies for detecting pressure instabilities, customary of turbomachinery, are based on piezoelectric effect used in high frequency response pressure transducers (4), and condenser microphones (5, 6). The benefit in using this kinds of sensors is the high sensitivity in a large frequency range, i.e. from Hz to 20 kHz or even more. However aerodynamic instabilities have a frequency response typically lower than 100 Hz. In particular, rotating stall occurs at a frequency that is about half of the rotor frequency. This circumstance motivates the attempt to develop a low-cost sensing solution, following-up the recent development of electret-based measurement microphones exploiting the large diffusion of electret capsules in the multi-media markets (7). This line of work is here addressed by proposing the use of unconventional DIY sensors for unsteady pressure measurements based on a piezoresistive pressure transducer and a commercial dynamic microphone capsule based on the electromagnetic induction working principle.

The measurement chains were first tested in an acoustically insulated duct in order to characterise the DIY sensors with respect to a high sensitivity piezoelectric microphone base-line. The comparative validation is then completed on a low speed industrial axial fan test-rig in a fully reverberant acoustic condition.

Frequency- and time-domain analysis were carried out on the acquired signals, to compare the performance of measurement methodologies under scrutiny during stall detection. The signal processing includes the reconstructed phase space methodology to detect the non-linear dynamics of measured pressure signals, not recognisable in the visual inspection.

NOMENCLATURE

BPF	Blade Passing Frequency [Hz]
DIY	Do It Yourself
FFT	Fast Fourier Transform
n	Index of row vortex
Q	Embedding dimension
RPS	Reconstructed Phase Space
τ	Time delay
x(n)	Scalar time series

$x(n+\tau)$ Lagged scalar time series

METHODOLOGY

Pressure transducer

The piezoresistive pressure transducer is an integrated silicon pressure sensor on-chip signal conditioned, temperature compensated and calibrated. It is a piezoresistive transducer that provide an analog output signal proportional to the applied pressure. The pressure range is -2 to 2 kPa (-0.3 to 0.3 psi), the output is 0.5 to 4.5 V. In Table 2 are listed the pressure transducer specifications. Figure 1 shows the cross sectional diagram of the pressure sensor and the differential configuration on the basic chip carrier.

Table 1 – Pressure transducer specifications (Differential configuration)

Typical error with auto zero	2.5% (over +10°C to +60°C)
Maximum error without auto zero	6.25% (over +10°C to +60°C)
Sensitivity	1.0 V/kPa
Time response	1.0 ms
Maximum pressure (P1 > P2)	75 kPa

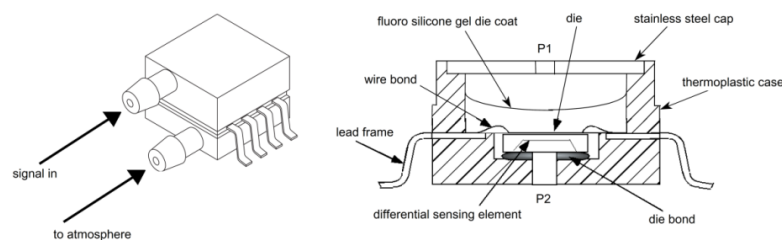


Figure 1 – Pressure sensor and its cross sectional diagram (not to scale)

The decoupling circuit showed in Figure 2 is needed for interfacing the integrated sensor to the A/D input, and to comply with the sensor specifications.

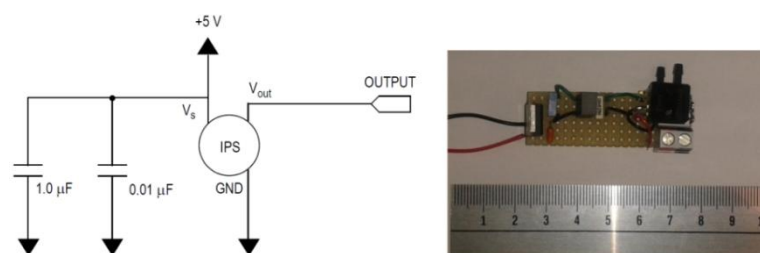


Figure 2 – On the left: power supply decoupling and output filtering; on the right: pressure transducer final layout

Dynamic microphone

The DIY microphone used in the present study is a commercial dynamic microphones. Table 3 gives the microphone characteristics.

Table 2 – Microphone specifications

Impedance	600 $\Omega \pm 30\%$
Sensitivity	-72 ± 3 dB
Frequency response	60 - 14 kHz

The dynamic microphone operation is based on the electromagnetic induction: the motion of the internal components of the microphone, generates a current output. The incoming sound pressure wave displaces a thin diaphragm, wrapped with a conductive wire coil surrounded by a magnetic field. The output is a voltage signal directly proportional to the sound pressure wave magnitude. The dynamic response is lower and the frequency response is less regular than ribbon or condenser microphones. Dynamic microphones are used in harsh working conditions and high noise level, due to their resistance. As much it is considered as a solution to measure hydrodynamic pressure in the near-field of a staving equipment. Figure 3 shows the microphone capsule and its design concept.

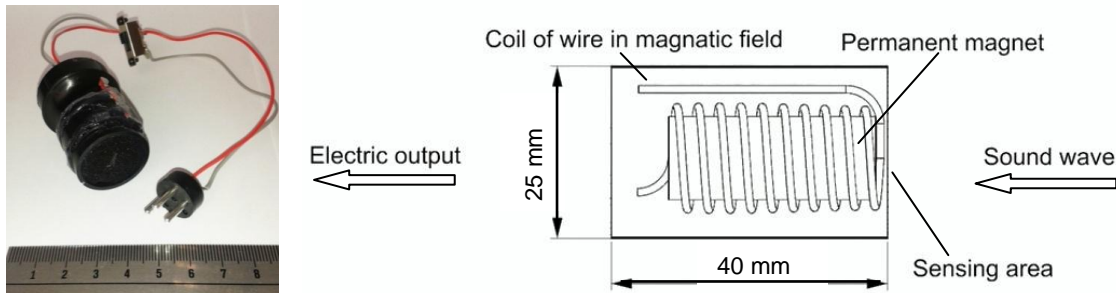


Figure 3 – The dynamic microphone

Operational amplifier

The pressure transducer and the dynamic microphone needed to be amplified. The amplifier circuit is based on the TL082 Op-Amp arranged in a non-inverting architecture. The amplifier circuit showed in Figure 4 is powered by two 9V batteries. A 10 kOhm linear potentiometer is set to the most suitable impedance for the connected sensor.

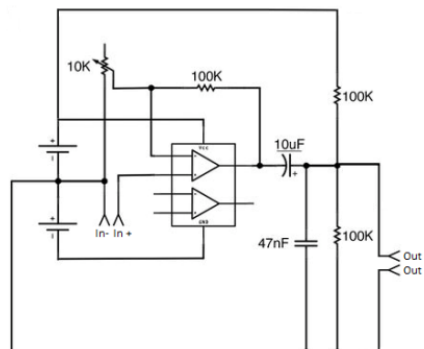


Figure 4 – The amplifier circuit

Piezoelectric microphone

The base-line probe is a high precision pre-amplified piezoelectric condenser microphone calibrated and certified according to the ISO-9001. When used on a fan test rig the piezoelectric microphone is usually placed in the far field. In Table 3 are showed the piezoelectric microphone characteristics.

Table 3 – Piezoelectric microphone specifications

Nominal microphone diameter	1/2"
Open circuit sensitivity (at 250 Hz)	12.5 mV/Pa
Open circuit sensitivity (± 2 dB) (at 250 Hz)	-38.1 dB re 1 V/Pa
Frequency range (± 2 dB)	4 to 20000 Hz

PROBE CHARACTERISATION TEST-RIG

To characterise the unconventional pressure transducers with respect to the piezoelectric microphone a measurement chain has been realized of which the transducer and the microphone constitute the final step. The authors used an an-echoic rig with a termination equipped with a sound source. The signals analysed are sine waves produced by a function generator; a set of frequencies were selected as the one closest to the pure tones of interest in the investigated axial fan. Figure 5 shows the layout of the characterisation rig.

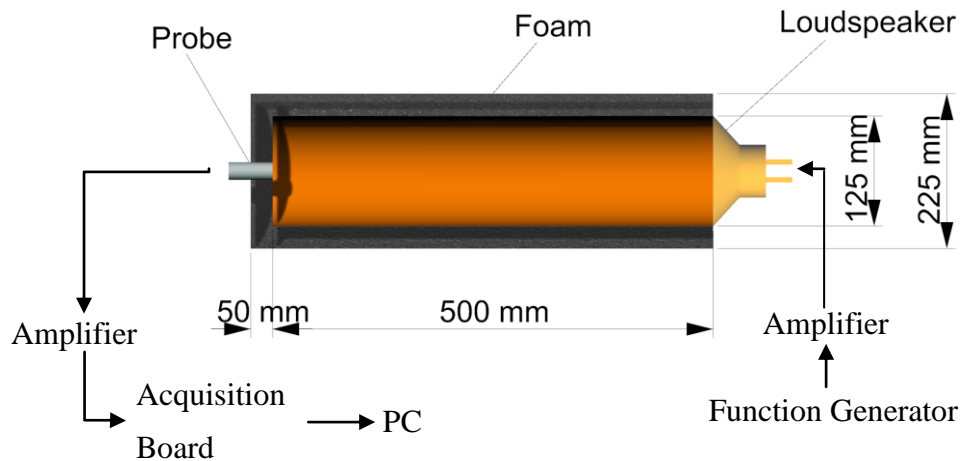


Figure 5 - Characterisation test-rig

The an-echoic tube was realised with a PVC duct with diameter 125 mm and length 500 mm. The duct was wrapped with foam to insulate it from the external noise. At one of the duct ends was placed a loudspeaker with impedance of 8 Ohm and maximum diameter of 125 mm. The loudspeaker was connected to the function generator. At the other end was placed a foam termination with inserted the pressure transducer and the piezoelectric microphone.

Function generator

The function generator is a testing instrument. The typical outputs are sine waves and the frequency and amplitude were regulated according to the needs. The frequencies used are the typical ones for the axial fan available for the authors. The function generator technical parameters are listed in the following Table 4.

Table 4 - Function generator technical parameters

Frequency range	0.2 Hz ~ 2 MHz
Output signal impedance	50 Ω
Output signal amplitude (peak-peak value)	non-attenuate (2 V _{p-p} ~ 20 V _{p-p}) \pm 20% *
	attenuate 20dB (0.2 V _{p-p} ~ 2.0 V _{p-p}) \pm 20% *
	attenuate 40dB (20 mV _{p-p} ~ 200 mV _{p-p}) \pm 20% *
Output signal features	sine wave distortion <2% **
Output signal frequency stability	less than \pm 0.1% /min **
Measurements errors	\leq 0.5%

* Continuously adjustable, **Test condition: frequency output 10kHz, amplitude: 5V_{p-p}, warm-up for 20 minutes

Signal amplifier

A signal amplifier is been placed between the function generator and the loudspeaker in order to compensate the loudspeaker low impedance and avoid a damage in the function generator. The amplifier circuit used is based on a TDA2003, capable of delivering 4 W_{rms} at 4 Ohms. The IC is thermally and short-circuited protected. The amplifier is designed to operate with the specifications in the following Table 5. In Figure 6 is showed the amplifier circuit.

Table 5 – Signal amplifier specifications

Output power	7W / 4 Ohm
RMS output power	3.5 W / 4 Ohm or 2 W / 8 Ohm
Total harmonic distortion	0.05 % (1 W / 1 kHz)
Frequency response	20 Hz - 20 kHz (-3 dB)
Input sensitivity	40 mV / 150 kOhm
Signal/noise ratio	86 dB (A weighted)
Power supply	8 - 18 VDC / 0.5 A
Dimensions	55 x 35 mm (2.2" x 1.4")

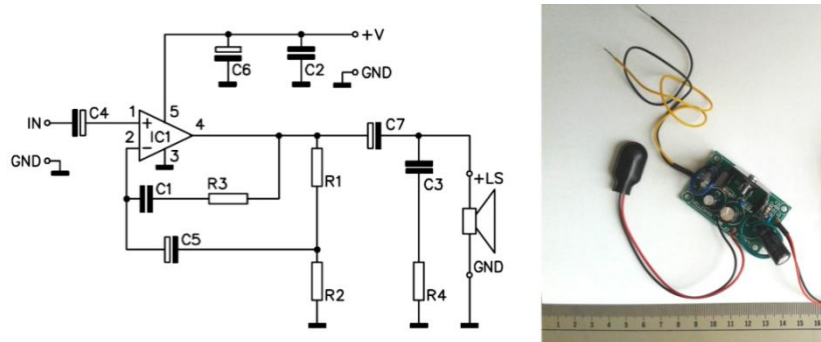


Figure 6 – The amplifier circuit

AXIAL FAN TEST-RIG

Axial fan specification

The turbomachine used for the experimental tests is a low speed industrial fan. Table 6 shows the specifications for the fan.

Table 6 – Fan data

Nominal speed	1000 rpm
Tip speed	40.6 m/s
Internal duct diameter	800 mm
Blades count	6
Blades length	200 mm
Tip clearance	5 mm
Blade chord at the tip	125 mm

A 1.55 kW direct coupled-induction 3-phase motor was used to drive the rotor at a constant speed of 100 rpm. Under these circumstances the blade passage frequency (BPF) for the tested configuration was 100 Hz, and the rotor frequency 16 Hz. The test rig airway is set according to the type-D configuration ISO 5801:2007 (8). The fan was driven to stall by throttling at the upstream end of the duct.

Instrumentation set-up

The fan rotor casing was instrumented with two inserts containing a pressure transducer and a dynamic microphone. The piezoelectric microphone was placed at 1 m distance from the fan casing, normal to the fan rotor. The probe arrangement is illustrated in Figure 7.

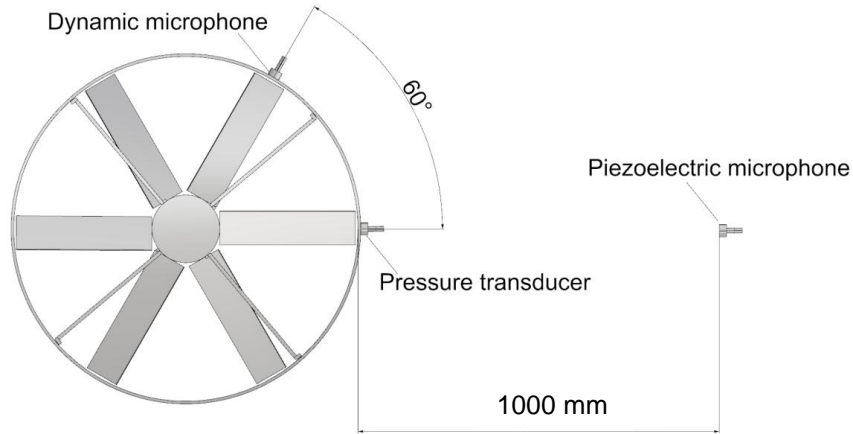


Figure 7 – Position of the sensors

The tests sampling time interval was 60 seconds with a sample frequency of 24 kHz, which is the acquisition board limit. In order to have significant acquired signals, it is been necessary to amplify the instruments. The experimental procedure was to provide a reduction of the flow rate through a throttle upstream the rotor, starting from a stable work condition until reaching the rotating stall.

SIGNAL PROCESSING

The signal processing includes a frequency-domain analysis based on Fast Fourier Transform (FFT), and a time-domain analysis based on the Reconstructed Phase Space (RPS) portraits.

The spectral analysis provides information about the power distribution over the frequency. To evaluate the spectrum of a temporal signal, the Fast Fourier Transform is implemented. The time signal is not continuous but discrete depending on the acquisition sample rate. The authors inspected the pressure signals through the spectral analysis in order to identify the frequency bands that reveal the rotating stall occurrence, as in the cross-correlation analysis already developed by Park (9).

The time-domain signal analysis was based on the Reconstructed Phase Space (RPS), following the stall detection through acoustic methods already investigated in Bianchi et al. (10) which proposed the use of symmetrised dot pattern representation of pressure sound signals in order to differentiate between critical and noncritical stall conditions, and to identify stall precursors. With the phase space reconstruction it is possible to do the embedding of an univariate sequence of data (the signal considered as a time series) in a reconstructed phase space (RPS) evaluating the time lag T and the embedding dimension D , so to obtain D vectors from the original signals using the T as the time delay (11). The RPS representation reads as:

$$\begin{bmatrix} \mathbf{x}_1 \\ \mathbf{x}_2 \\ \vdots \\ \mathbf{x}_t \\ \vdots \\ \mathbf{x}_{N-(D-1)T} \end{bmatrix} = \begin{bmatrix} x_1 & x_{1+\tau} & \cdots & x_{1+(D-1)\tau} \\ x_2 & x_{2+\tau} & \cdots & x_{2+(D-1)\tau} \\ \vdots & \vdots & \ddots & \vdots \\ x_t & x_{t+\tau} & \cdots & x_{t+(D-1)\tau} \\ \vdots & \vdots & \ddots & \vdots \\ x_{N-(D-1)T} & x_{N-(D-2)T} & \cdots & x_N \end{bmatrix} \quad (1)$$

The RPS allows the identification of the characteristics contained in the non linear dynamic systems, which are not identifiable with the time domain analysis of the single signal. The accurate reconstruction of the phase space depends on the definition of D and T . The optimal time delay T is identified with the first minimum of the mutual information (12). The embedding dimension D , is identified with the false nearest neighbours method (13). The value of D is 2 in every case. The value of T used, in the present investigation, are summarized in Table 7. Notably, the indicated periods are representative of 10 signal oscillations for each of the analysed frequencies.

Table 7 – Periods and time delay used in the investigation

Frequency	Period	Time delay (T)		
		Dynamic	Piezoelectric	Pressure
8	1.25	1	2	2
16	0.625	2	2	6
100	0.1	5	5	6

RESULTS

Figures 8, 9 and 10, respectively, illustrate the visual inspection of the signals acquired in the characterization test-rig with the pressure transducer, the dynamic microphone and the piezoelectric microphone. The sinusoidal signals were acquired at four frequencies that are the most representatives for the axial fan, namely the rotating stall frequency 8 Hz, the rotor frequency 16 Hz and the BPF 100 Hz.

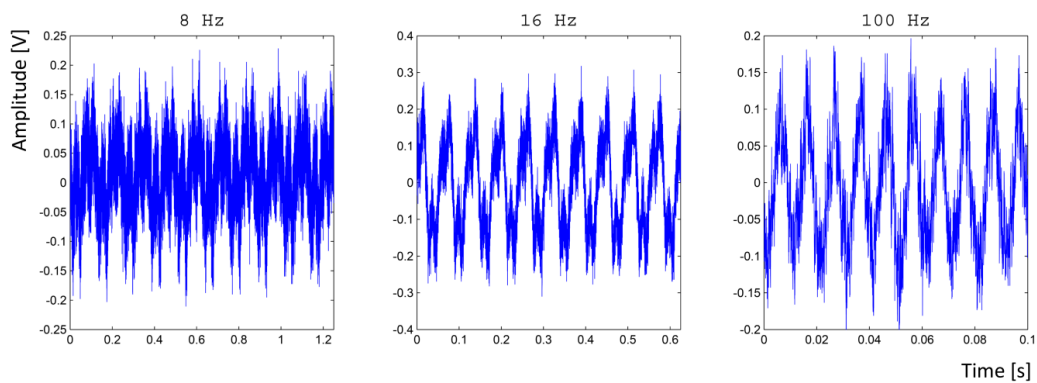


Figure 8: Sound generator signals acquired with the pressure transducer at 8 Hz, 16 Hz, 100 Hz

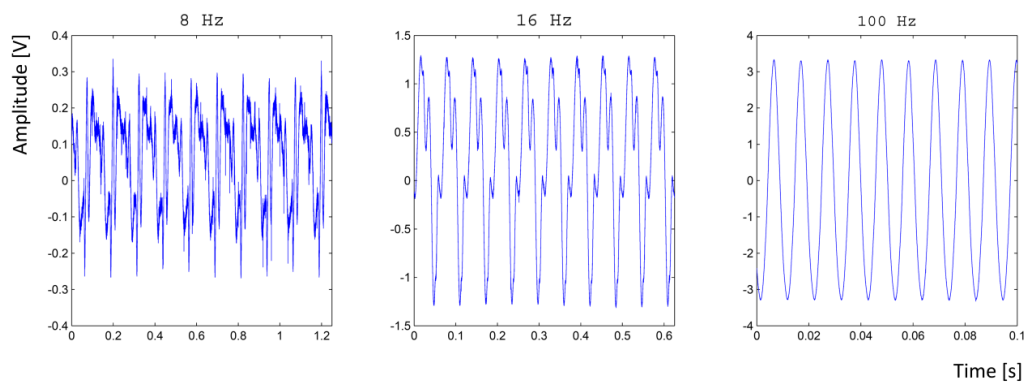


Figure 9: Sound generator signals acquired with the dynamic microphone at 8 Hz, 16 Hz, 100 Hz

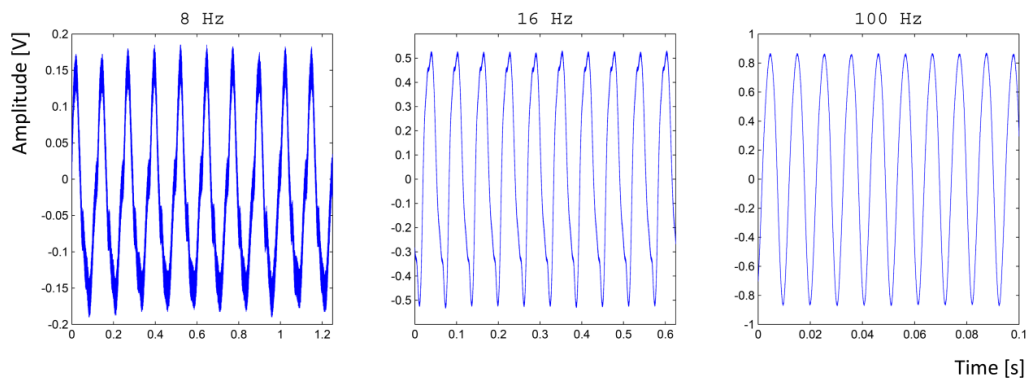


Figure 10: Sound generator signals acquired with the piezoelectric microphone at 8 Hz, 16 Hz, 100 Hz

The comparative visual inspection demonstrates that the pressure transducer gives a disturbed signal at very low frequencies as well as at the higher ones. The dynamic microphone signal, which shows a behaviour very comparable to the piezoelectric microphone one at the higher frequency, is able to reconstruct the sinusoidal response even at the lowest frequency, in the test 8 Hz. In contrast the reference probe, clearly, outperforms to two DIY technologies with small distortions.

Axial fan analysis

The pressure signals have been acquired at a sample frequency f_S of 24 kHz, corresponding to a Nyquist frequency f_N of 12 kHz. The sample frequency was chosen in accord to the acquisition board characteristics used to acquire concurrently the signals of two probes.

Figure 11, first, shows the signals acquired with the two sensors near-field sensors and the far-field microphone. The two top pictures represent the signal time traces measured by the pressure sensor and the dynamic microphone, while the bottom one illustrates the signal time trace measured by the reference piezoelectric microphone.

The spectral and the RPS analyses have been applied over a time window of 1 s, equivalent to approximately 16 rotor revolutions, selecting operating conditions which are representative of stable and stalled operations. The time windows have been taken in the stable and in the stalled region of the acquired signals.

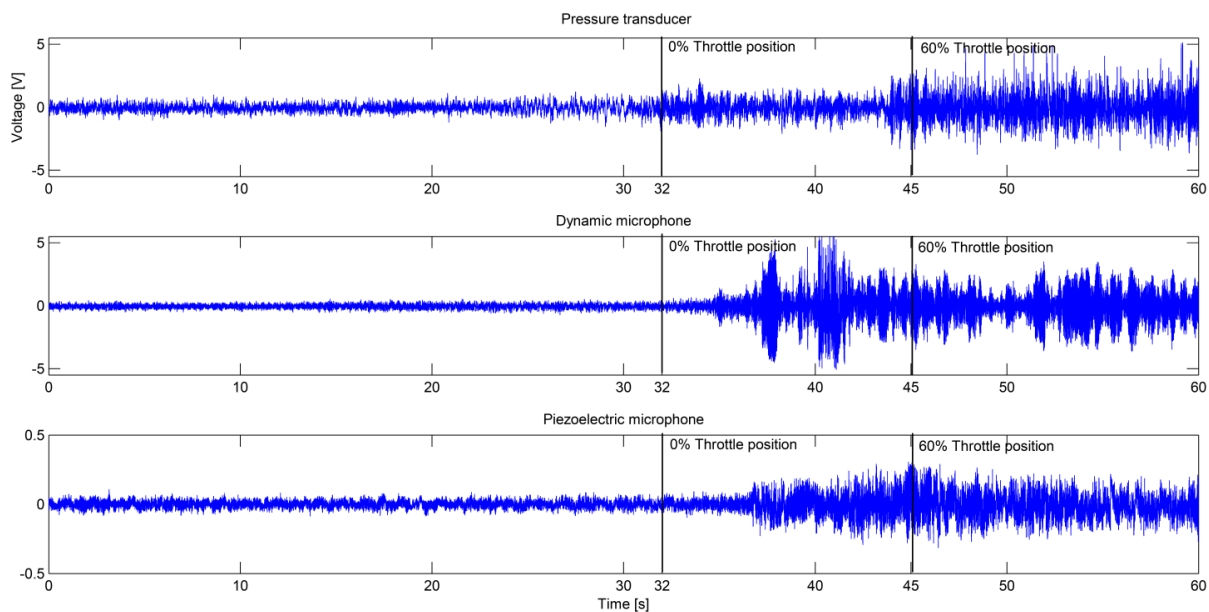


Figure 11 – The axial fan acquired signals in time domain

Moreover, Figure 12 illustrates the auto-spectra of the signals measured by the pressure transducer (Figure 12.a), the dynamic microphone (Figure 12.b) and the piezoelectric microphone (Figure 12.c) during, respectively, the stable and stalled work condition.

When looking at the DIY probes spectra, it is remarkable that their response in the frequency range above the first harmonic of the BPF is attenuated. This circumstance, in general true at stable operations for the DIY spectra, applies also with the fan operated at stall. In this condition, the DIY sensors appeared to give rise to a much richer spectral signature but in the limit of the low frequency range much affected by the emergence of rotating instabilities (stall) tones at about 50% of the rotor frequency (i.e. 16 Hz). In this respect the far-field piezoelectric probe, is able to resolve all the frequency components in the sound radiated from the test-tube in a reverberant environment.

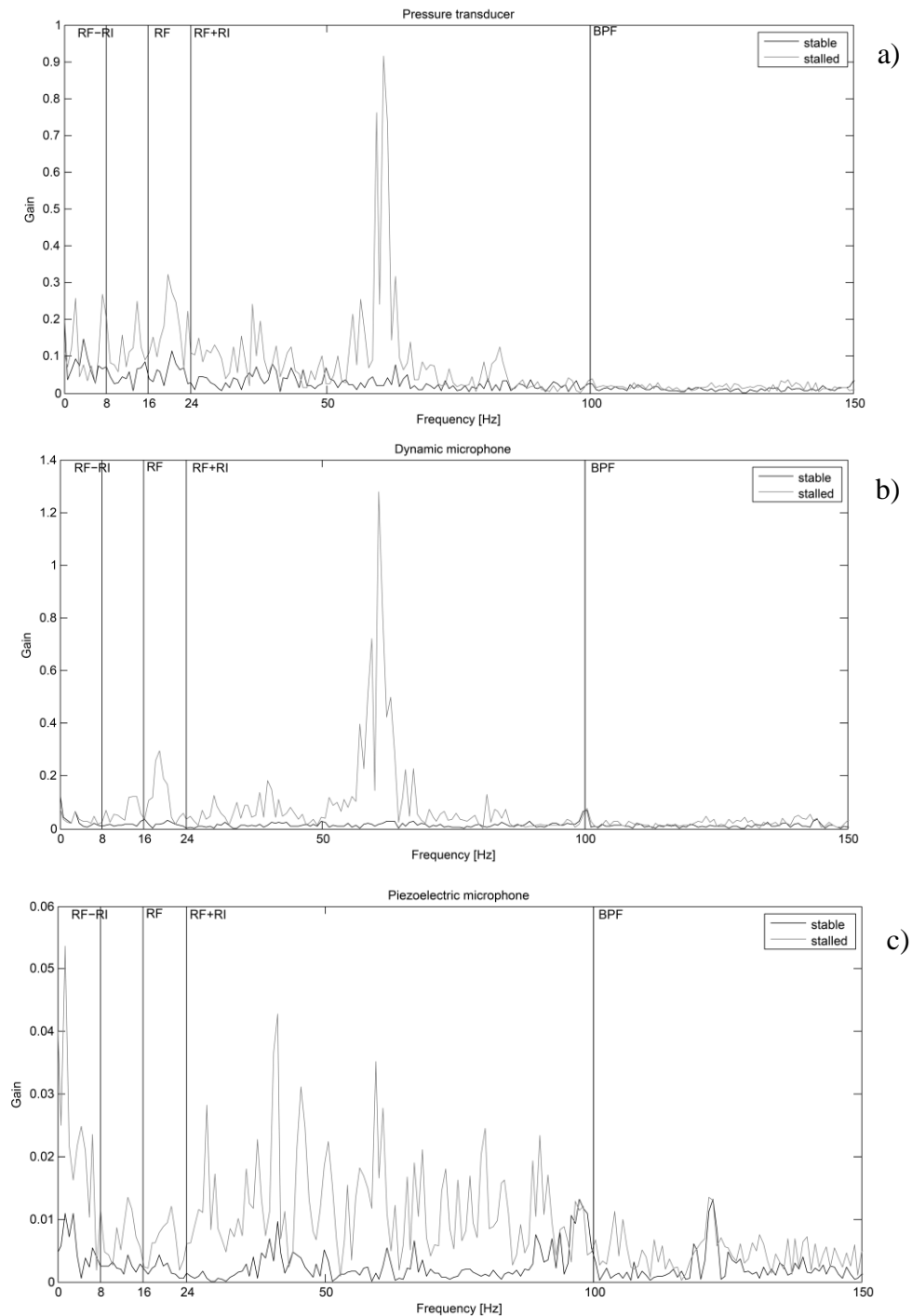


Figure 12: Spectral analysis for stable and stalled work condition of: a) the pressure transducer, b) dynamic microphone and c) piezoelectric microphone signals

Phase-space portraits RPS

Figure 13 shows the evolution of the RPS starting from a stable operating condition towards the aerodynamic instability for the signal acquired with the pressure transducer. The stable condition corresponds to the time interval 1÷2 s, the stalled condition correspond to the time interval 45÷46 s of the first signal in Figure 11.

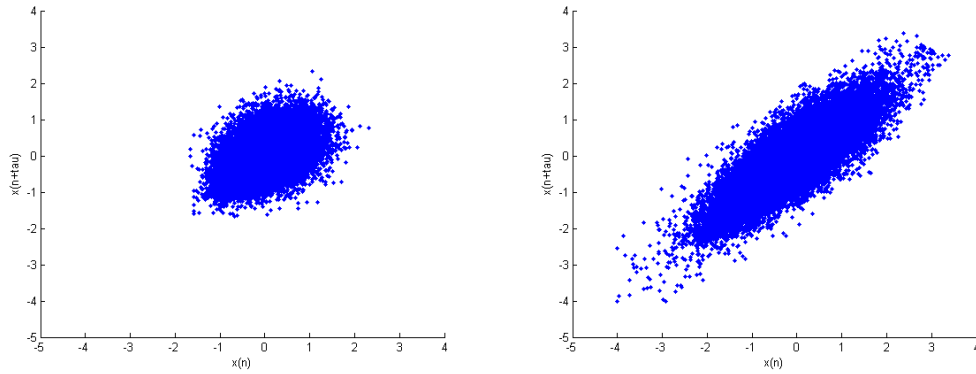


Figure 13 – On the left the stable operation, on the right the stalled operation for the pressure transducer

Figure 14 shows the evolution of the RPS starting from a stable operating condition towards the aerodynamic instability for the signal acquired with the dynamic microphone. The stable condition corresponds to the time interval 1÷2 s, the stalled condition correspond to the time interval 45÷46 s of the middle signal in Figure 11.

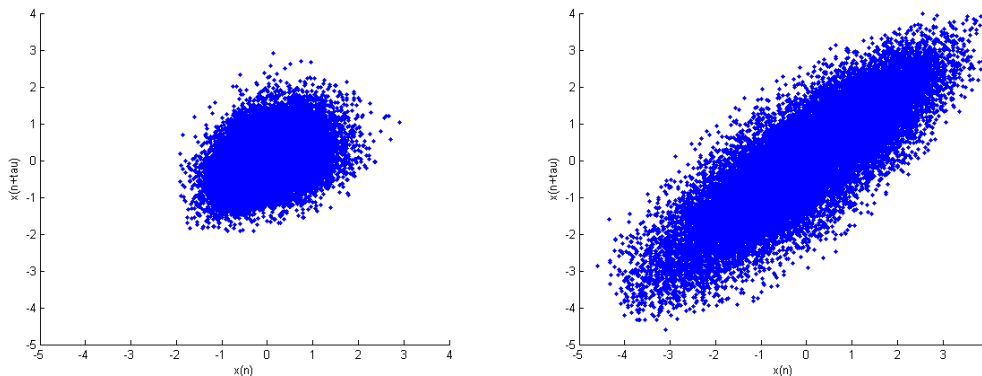


Figure 14 – On the left the stable operation, on the right the stalled operation for the dynamic microphone

Concerning the piezoelectric microphone, it was placed in the far field at 1 m from the fan casing. Figure 15 shows the evolution of the RPS starting from a stable operating condition towards the aerodynamic instability for the signal acquired with the piezoelectric microphone. The stable condition corresponds to the time interval 1÷2 s, the stalled condition correspond to the time interval 45÷46 s of the middle signal in Figure 11.

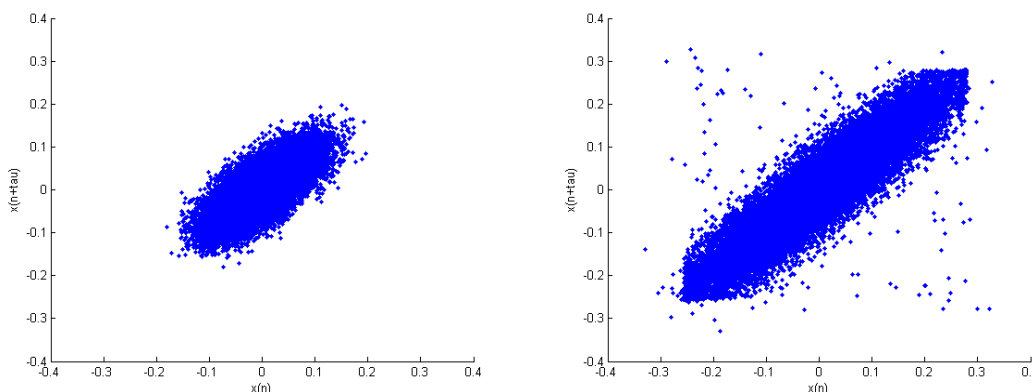


Figure 15 – On the left the stable operation, on the right the stalled operation for the piezoelectric microphone

Notably, in addition to the evidence of the spectral analysis, the portrait comparison indicates that both the signals from the pressure transducer and the dynamic microphone are able to create phase-space patterns which identify sharply the evolution from stable to stalled operations. The signature of such evolution being the diagonal stretching of patterns and, as already explained, this circumstance could be correlated with the predominance at stall of a chaotic behaviour with the

orbits of RPS attractor evolving in a complex shape; whereby some directions are contracted and other are stretched.

CONCLUSIONS

From the frequency domain analysis through the Fast Fourier Transform is noticeable that rotating stall occurs at low frequencies, lower than 100 Hz; more importantly the rotating stall is visible with both the DIY instruments. The clearly visible frequency peak at 64 Hz during stalled operations is considered to be a resonant frequency due to the rotor-strats interaction. The experiment proves that the dynamic microphone is able to detect the presence of aerodynamic instabilities at frequencies lower than 20 Hz with a 50 ÷ 60 % precision. Indeed applying the Spectral Analysis on the dynamic microphone signal, it is possible to detect a peak at about 15 Hz which is near the value 16.2 Hz of the rotor frequency. Using the RPS method the authors identified the rotating stall typical pattern. As in the Spectral Analysis, the method response is more chaotic, and the pattern tends to enlarge and extend while approaching the unsteady condition.

Both the pressure transducer and the dynamic microphone have detected the presence of the rotating stall phenomenon, and the analysis methods used confirmed the validity of the used instruments.

However from the RPS analysis of the sine wave signals, it is especially for the lower frequency, how the dynamic microphone works better than the pressure transducer, if the piezoelectric microphone is taken as a reference. And this is confirmed in the RPS analysis, where it is visible the similarity between the dynamic and piezoelectric microphone system response.

REFERENCES

- [1] Bianchi S., Corsini A., Sheard A. G., Tortora C. – *A Critical Review of Stall Control Techniques in Industrial Fans*, ISRN Mechanical Engineering, Volume **2013**, Article ID 526192
- [2] Cumpsty N. A. – *A critical review of turbomachinery noise*, J. of Fluids Engineering, pp. 278-293, **1977**
- [3] Cumpsty N. A. – *Sum and difference tones from turbomachines*, Journal of Sound and Vibration, Vol. 32/3, pp.383-386, **1974**
- [4] Bianchi S., Corsini A., Mazzucco L., Monteleone L., Sheard A. G. – *Stall Inception, Evolution and Control in a Low Speed Axial Fan With Variable Pitch in Motion*, Journal of Engineering for Gas Turbines and Power APRIL **2012**, Vol. 134 / 042602-1
- [5] Bianchi S., Corsini A., Sheard A. G. – *Detection of stall regions in a low-speed axial fan. Part i - azimuthal acoustic measurements*, Proceedings of ASME Turbo Expo **2010**, GT2010-22753
- [6] Zhu T., Carolus T.H. – *Experimental and unsteady numerical investigation of the tip clearance noise of an axial fan*, Proceedings of ASME **2013**, TBTS2013-2043
- [7] Gareth J. Bennett, Mahon, J., Hunt, S. & Harris, C. – *Design of an Electret Based Measurement Microphone*, in 26th International Manufacturing Conference (IMC26) 411–418, **2009**
- [8] ISO 5801, **2007** – *Industrial Fans—Performance Testing Using Standardized Airways*
- [9] H. G. Park – *Unsteady disturbance structures in axial flow compressor stall inception [M.S. thesis]*, Massachusetts Institute of Technology, Cambridge, MA, USA, **1994**
- [10] S. Bianchi, A. Corsini, and A. G. Sheard – *Demonstration of a stall detection system for induced-draft fans*, Journal of Power & Energy, **2013**
- [11] Abarbanel HDI, Brown R, Sidorowich JJ, Tsimring LS. – *The analysis of observed data in physical systems*, Reviews of Modern Physics, Vol. 65, No. 4, October **1993**, p.1343-51

[12] Gallager R. – *Information Theory and Reliable Communication*, **1968**

[13] Kennel M.B., Brown R., Abarbanel H.D.I. – *Determining embedding dimension for phase space reconstruction using a geometrical construction*, Physical review A, Vol 45, No 6, 15 March **1992**, pp.3403-3411